inter.noise
HAMBURG 2016

Modeling of Non-linear damper for suppression of micro vibration on a car body

Hiroki NAKAMURA[1], Toshiaki KAMO[2], Hideki OHSAWA[3], Hiroshi SAKANOUE[4], Toru YAMAZAKI[5]

[1, 5] Kanagawa University, Japan

[2, 3, 4] Yamaha Motor Co., Ltd, Japan

ABSTRACT

The present damper developed for a micro vibration suppression of a car body, that uses an oil hydraulic pressure control valve for generating damping force, is able to produce a velocity-independence nearly constant damping force unlike an ordinary viscous damper and hence to produce a large damping force in a very small velocity range. However, a particular account of the generation mechanism of a damping force has not been given so far.

This paper presents firstly the derivation of equation for attenuation characteristics; nonlinearity of the present damper with a built-in oil hydraulic pressure control valve as an attenuation mechanism. Next, linear attenuation coefficient equivalent to the non-linear damping force is driven using a describing function method and then the validity of modeling of damping mechanism and its linearization technique is verified on the basis of comparison of simulations with experiments.

Keywords: Modeling, Non-linear damper, Automobile I-INCE Classification of Subjects Number(s): 47.1

1. INTRODUCTION

Reduction of automobile frame vibration is highly demanded due to better comfort, agility and maneuverability. However, conventional viscus dampers does not work effectively on frame vibration because its amplitude is very small. Then, non-linear damper for suppression of micro vibration on a car body (also called performance damper) is developed; it produces a velocity-independence nearly constant damping force. An installed performance damper is shown in fig.1. As shown in fig.1, the damper is usually installed to bridge two longitudinal frames and also another damper is installed parallel in front. Two dampers suppress frame vibration realizes desired performance. However, the quantitative analysis of the dampers characteristics is not examined yet because the detailed model of the damper is not established.

Figure 1 – Performance damper installed on a car

[1] hiroki-nak@kanagawa-u.ac.jp
[2] kamoto@yamaha-motor.co.jp

This research aim on establish of optimize design process of automobile frame damping characteristics. For the first step of the research, modeling of non-linear damper for suppression of micro vibration on a car body is reported. At beginning, vibration suppression mechanism of the target damper is clarified. Then, validity of dynamic model of the target damper is examined through theoretical analysis and excitation experiment.

2. CHARACTERISTICS OF TARGET PERFORMANCE DAMPER

2.1 Main components of target performance damper

Main components and structure of target performance damper and shown in fig. 2.

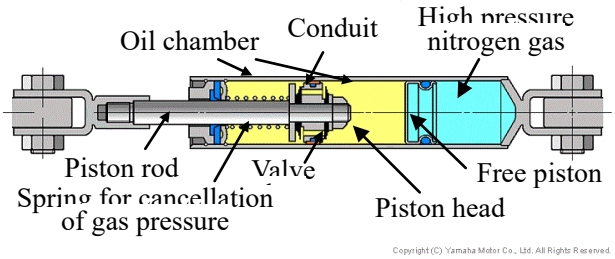

Figure 2 – Components of test performance damper

Pressure control valves work as damping elements, which is composed of several conduits and disk valve plates. The level of damping force is designed by changing the disk characteristics: diameter, thickness, and numbers.

Also, oil chamber is pressured by high pressure nitrogen gas via free piston, so to prevent drop of bulk modulus. This structure restrains response lag caused by volume effect during very small excitation. Additionally, spring for cancellation of gas pressure enables easy installation on a car.

2.2 Damping Force Characteristics

Damping force characteristics of test dampers are shown in fig.3; lateral and vertical axis represents velocity and damping force respectively. This characteristics resembles pressure vs flow rate characteristics of linear relief pressure valve; rise to constant damping force based on cracking pressure and small elevation of damping force proportional to velocity caused by pressure override. The figure shows that target dampers can generate strong damping force from very small velocity unlikely to conventional velocity proportional viscus dampers.

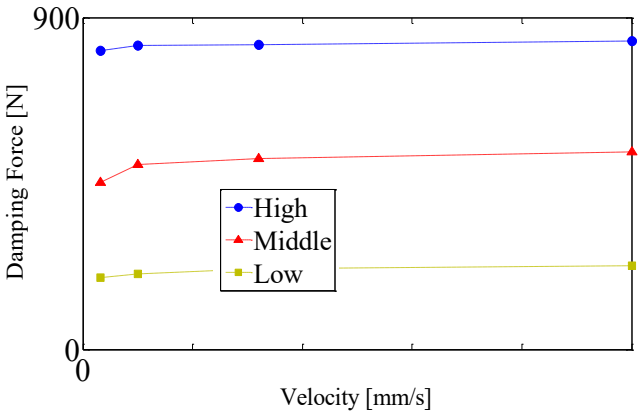

Figure 3 – Measurements of the damping force vs piston speed characteristics of test dampers

3. METHODOLOGY

3.1 Modeling of slide motion of the target damper

Equation of motion of the target damper is expressed as following eq.1 with assumption that the cylinder is fixed and the piston rod is excited with sinusoidal force $f(t)$; m, x, k, and F represent mass of the piston rod, displacement of the rod, stiffness of the spring cancellation for high pressure gas, and damping force respectively. Here, right-face positive in fig.2 for displacement and force. In practical term, damping force against relative velocity of piston and cylinder should be considered because cylinder is also excited. To focus on clarification of damping force generating mechanism and its modeling, above assumption is premised in this report.

$$m\frac{d^2x}{dt^2} + F + kx = f(t) \tag{1}$$

3.2 Modeling of damping force generated by pressure control valve

In general, pressure control valve, or linear pressure relief valve in detail, shows flow rate vs pressure difference characteristics as shown in fig.4. Pressure difference means pressure gap of oil between two sides of valve. In the fig.4 cracking pressure p_c and Δp is also described.

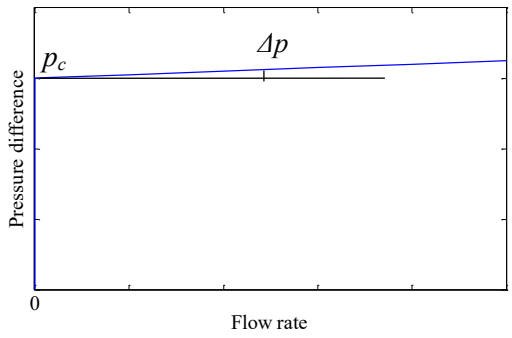

Figure 4 – General characteristics of pressure control valve

Characteristics of pressure control valve shown in fig.4 resembles velocity vs damping force characteristics of the target damper. It suggests that the damping force F of the target damper is generated by pressure drop (or difference) when oil flows through the orifice of pressure control valve. Thus, correlation between sliding velocity dx/dt and damping force F can be derived if correlation between flow rate Q and pressure difference p is solved, and damping mechanism of target damper is clearly described.

Figure 5 shows detailed structure of the pressure control valve which is composed of several conduits and a disk valve plate, mentioned in section 2.1. In following paragraphs, derivation of equation of damping force generated by the structure shown in fig.5 (or the model of the target damper) is mentioned.

Here, several conditions are assumed.

(1) Pressure of oil chamber of the left side (piston head side) is independent of the motion of piston and it is at the same level as gas pressure P_0.

(2) Pressure of oil chamber of the right side (cylinder side) is amount p higher (when dx/dt is greater or equal 0) or lower (when dx/dt is less or equal 0) than the pressure of oil on piston head side; p represents pressure drop at pressure control valve.

(3) Damping force F is mostly generated by the pressure drop p, and other factors such as friction of oil seal are neglected.

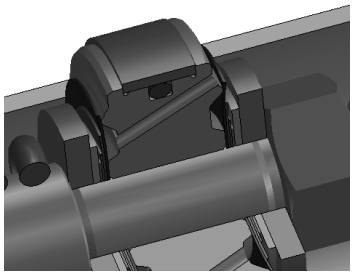

Figure 5 – Valve plate structure for pressure control valve with a built-in test damper

Definition of each symbol used in following equations are shown in table 1.

Table 1 Symbol and term of parameters for pressure control valve

Symbol	Term
n	Number of valve (flow path)
x_v	Valve opening
θ	Discharge angle from the valve
ρ	Density of the fluid
Q	Flow rate
C_d	Discharge coefficient of the valve
D	Diameter of the conduit

Schematic image of operating pressure control valve in the target damper is shown in fig.6. Here, top half represents the operation while piston is moving right, and oil flows through conduit from the right. Bottom half represents vice versa.

Equilibrium of force is expressed as eq.2 when the piston is sliding at the constant velocity (positive or negative). Pressured area on both sides of valve is defined as A_h and A_r (suffix for head and rod); stiffness of the spring for cancellation of gas pressure is defined as k; and initial displacement of piston is defined as x_0.

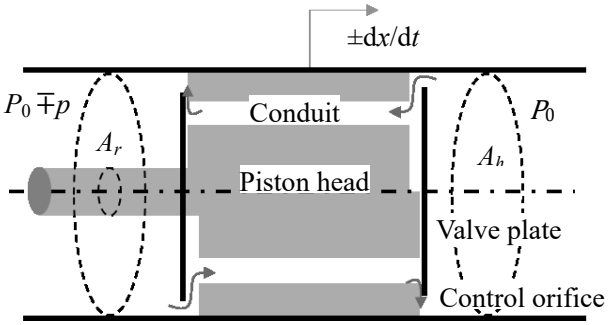

Figure 6 – Modeling of pressure control valve for generating constant damping force

$$-k(x-x_0)+A_r(P_0\mp \qquad {}_0^{\cdot}=0 \tag{2}$$

If the piston is standing still, eq.3 is deduced.

$$kx_0 + A_r P_0 - A_h P_0 = 0 \tag{3}$$

Thus, damping force F mentioned in eq.1 is described as follows.

$$\frac{dx}{dt} > 0 : F = A_r p \tag{4}$$

$$\frac{dx}{dt} < 0 : F = -A_r p \tag{5}$$

Here, eqs. 4 and 5 can be united as follows.

$$F = \mathrm{sgn}\left(\frac{dx}{dt}\right) A_r p \tag{6}$$

Next, correlation between flow rate Q and pressure difference p is derived. Schematic image of oil flow around orifice of plate-type pressure control valve is shown in fig.7, which is functionally same as pressure control valve shown in fig.6.

Flow rate Q is derived as follows from equation of orifice in fluid dynamics.

$$Q = nC_d \pi D x_v \sqrt{\frac{2p}{\rho}} \tag{7}$$

Here, flow coefficient C_d is a variable according to Reynolds number and valve output, but practically a constant between 0.65 and 0.7 is used.

Then, equilibrium of force around valve plate is expressed as follows; k_v, x_v, $x_{v.0}$, a, v, θ, and C_u stiffness of valve spring. Valve output, initial displacement of valve, pressured area, velocity of flow, flow angle (between horizontal axis), and velocity coefficients respectively. Second term on the left represents fluid force based on change of momentum.

$$ap - \rho v Q \cos\theta = k_v (x_v + x_{v.0}) \tag{8}$$

$$\therefore ap - 2\pi C_u C_d \sin\theta \cos\theta p x_v = k_v (x_v + x_{v.0}) \tag{9}$$

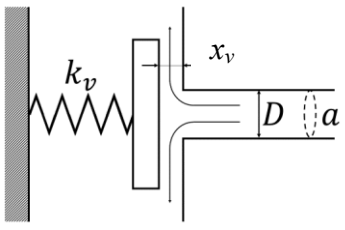

Figure 7 – Model of a plate–type pressure control valve

Here, angle of flow is approximately vertical to the conduit axis, so eq.9 can be simplified as follows.

$$ap = k_v (x_v + x_{v.0}) \tag{10}$$

Thus, pressure difference p can be described as the function of valve output x_v as follows

$$p - \frac{k_v(x_v + x_{v.0})}{a} = p_c + \frac{k_v x_v}{a} \tag{11}$$

Here, p_c is the pressure when the valve starts to move (or displacement x_v=0), and so called cracking pressure. Cracking pressure p_c solved as follows from eq.11.

$$p_c = \frac{k_v x_{v.0}}{a} \tag{12}$$

Also, relation between valve output x_v and pressure p is derived as follows.

$$x_v = \frac{ap - k_v x_{v.0}}{k_v} \tag{13}$$

Following equation of flow rate Q and pressure difference p is derived by substituting eq.13 for eq.7.

$$\begin{aligned} Q &\approx nC_d \pi D x_v \sqrt{\frac{2p}{\rho}} = nC_d \pi D \left(\frac{ap - k_v x_{v.0}}{k_v} \right) \sqrt{\frac{2p}{\rho}} \\ &= nC_d \pi D \frac{a}{k_v} (p - p_c) \sqrt{\frac{2p}{\rho}} \end{aligned} \tag{14}$$

As above, correlation between Q and p is non-linear, so it is difficult to grasp the tendency in quantitative manner. However, correlation similar to fig.4 can be derived by substituting known parameters like a, k_v, and ρ.

Correlation between damping force F and velocity dx/dt is deduced from equation of continuity as follows and eq.6. Thus, damping mechanism of the target damper is formulated.

$$Q = A_r \frac{dx}{dt} \tag{15}$$

3.3 Linearization of damping force

For theoretical analysis of damping performance of the target damper, damping force F is linearized in this section. Damping force F is approximated as follows with assumption that leakage at very low speed can be neglected and damping force stem from pressure override is proportional to piston speed (gradient coefficient: α).

$$F = \mathrm{sgn}\left(\frac{dx}{dt} \right) F_0 + \alpha \frac{dx}{dt} \tag{16}$$

Here, F_0 (=$A_r p_c$) is constant damping force stem from cracking pressure. Equation 16 can be illustrated as fig.8; Damping force rises (or drops) drastically to F_0 (or -F_0) around 0 [mm/s], and velocity proportional force with gradient α is added.

Then, sinusoidal excitation expressed as eq.17 is assumed, and damping characteristics is linearized with describing function technique and equivalent damping coefficients c_{eq} as eq.18 is derived.

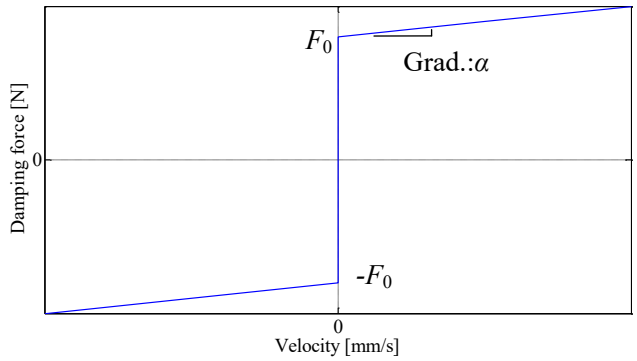

Figure 8 – Correlation between velocity and damping force

$$x = X_0 \sin \omega t \tag{17}$$

$$F \equiv c_{eq} \frac{dx}{dt} \tag{18}$$

Overview of linearization with describing function technique is described as follows. Characteristics mentioned above is point symmetry around dx/dt=0, so only condition dx/dt>0 is described and the other condition condition dx/dt<0 is omitted.

Assume that works of non-linear damping force shown in eq.16 and linear damping force shown in eq.18 are equal in one cycle of oscillation, which is described as following eq.19, equivalent damping coefficients are obtained as eq.20

$$\oint \left(F_0 + \alpha \frac{dx}{dt} \right) dx = \oint c_{eq} \frac{dx}{dt} dx \tag{19}$$

$$c_{eq} = \frac{4F_0}{\pi X_0 \omega} + \alpha \tag{20}$$

Thus, equation of motion for the target damper during sinusoidal forced excitation with amplitude f can be described as following linear equation.

$$m \frac{d^2x}{dt^2} + c_{eq} \frac{dx}{dt} + kx = f \sin \omega t \tag{21}$$

4. EXPERIMENT and DISCUSSION

4.1 Apparatus and Conditions

Sinusoidal excitation test of the target damper is performed with shock absorber tester. Apparatus is shown in fig.9. Conditions are shown below. Three types of the target dampers shown in fig.3 is measured in each conditions.

(a) Every 10Hz from 10Hz to 50Hz with amplitude 0.5mm; 5 conditions
(b) 4 amplitudes, 0.5mm, 0.7mm, 0.9mm, and 1.0mm with 10Hz and 20Hz; 8 conditions in total

Displacement of the piston slide is measured with an inductive displacement sensor. Damping force is measured with load cell installed on the edge of a cylinder. Temperature of the target dampers are controlled in allowable range to neglect the change of viscosity of oil inside.

Figure 9 – Sinusoidal excitation experimental equipment for test damper

4.2 Result of measurement

An example result of time historical displacement, velocity, and force are shown in fig.10 and fig.11; excited with 0.5mm amplitude and 40Hz. In this experiment, amplitude is very small so that stiffness of spring and inertia of piston could be neglected. It means that damping force is dominant in measured force. Historical data of fig.10 deviate from sinusoidal wave form near transition point (where velocity switches its direction).

Figure 12 is an example data of velocity vs damping force characteristics. Here, velocity is calculated by numerical substitution of displacement data. Damping force characteristics due to cracking pressure and pressure override are clearly drawn in the figure.

However, unlikely to the theoretical characteristics shown in fig.8, hysteresis is seen in fig.12 near transition point, where velocity shift its direction. This is mainly because first-order response lag of pressure inside caused by friction of free piston and compressibility of oil (including elasticity of the chamber); while piston is moving, pressure of cylinder P reaches the pressure of gas P_0 with time delay. Nonetheless, there are small influence on linearized equivalent coefficients because delay of expansion and contraction cancel each other.

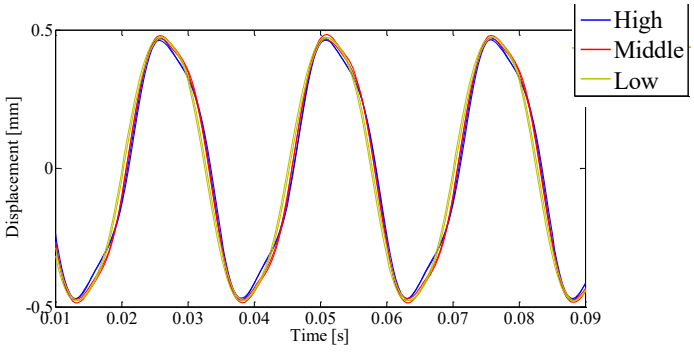

Figure 10 – Time history waveforms of displacement at 40Hz sinusoidal excitation of 0.5mm amplitude

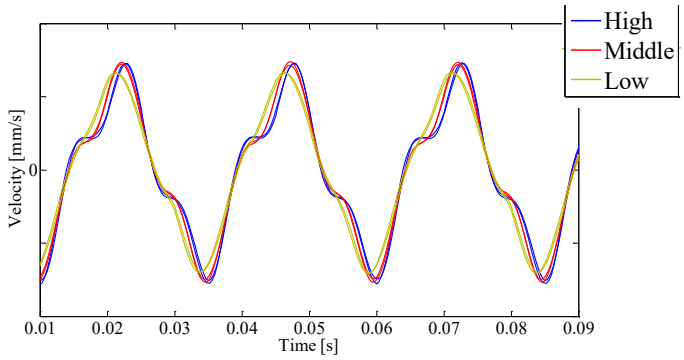

(a) velocity

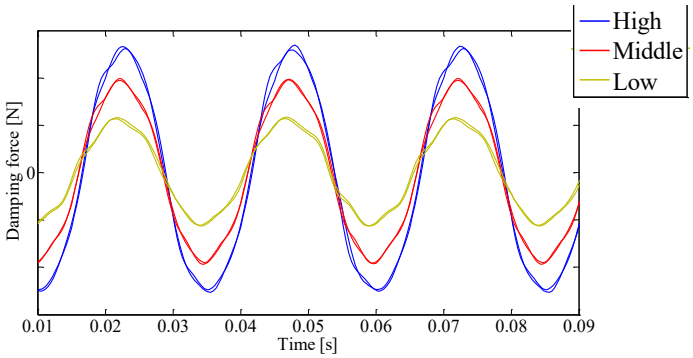

(b) damping force

Figure 11 – Time history waveforms of damping force at 40Hz sinusoidal excitation of 0.5mm amplitude

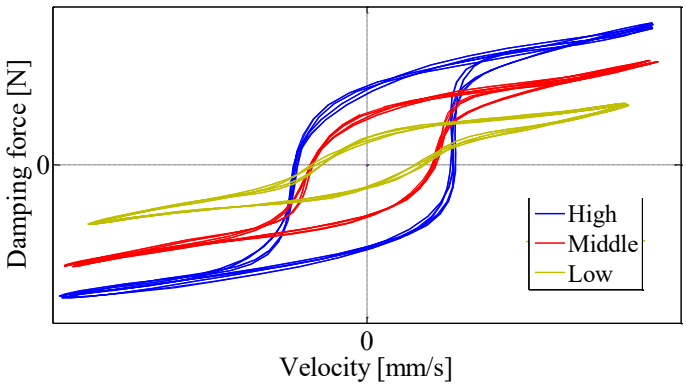

Figure 12 – Correlation between velocity and damping force

4.3 Discussions

Equivalent damping coefficient c_{eq} derived from model equation (Eq.20) and experimental data is compared in this section to check validity of the proposed model. Table 2 is the list of equivalent damping coefficients calculated with experimental data by least-square method; conditions with constant amplitude 0.5mm are shown.

Table2 Damping coefficients obtained from experimental data [Ns/m]

Type	Input frequency				
	10Hz	20Hz	30Hz	40Hz	50Hz
High	26921	15746	11385	9652	9005
Middle	19980	11421	8601	7435	7054
Low	10066	6068	4904	4410	4284

Table 3 is the list of equivalent damping coefficients of three types of target damper calculated with model equation; conditions with constant amplitude 0.5mm are shown.

Table3 Damping coefficient calculated by Eq. (20) [Ns/m]

	Input frequency				
	10Hz	20Hz	30Hz	40Hz	50Hz
High	31093	15895	10829	8296	6776
Middle	18878	9759	6719	5199	4288
Low	8731	4678	3327	2651	2246

Table 4 is the difference of equivalent damping coefficients between experiment and proposed model; difference rate is calculated based on experimental data and its root mean square values between 20Hz to 40Hz and 10Hz to 50Hz are both shown.

Table4 Relative error between experiment and proposed model

Type	Difference RMS[%]	
	20～40Hz	10～50Hz
High	8.60	14.7
Middle	23.1	25.2
Low	32.4	33.4

Note that response lag become unneglectable at high frequency and the exciter can not provide accurate sinusoidal force at low frequency, so RMS of 20Hz to 40Hz are evaluated and RMS of 10Hz to 50Hz are only reference value.

There is room for improvement on this model by considering response lag. It will be discussed in further report. Nonetheless, maximum value of error RMS is within reasonable range in all conditions at this point.

5. CONCLUDING REMARKS

In this research, modeling of non-linear damper for suppression of micro vibration on a car body is reported. Summary of the research is as follows.

(1) Damping mechanism of the target damper is clarified that pressure control valve composed of a disk conduits on piston head enables generation of nearly constant damping force. The mechanism is illustrated by dynamical model and its validity is examined excitation test.

(2) Non-linear damping characteristics is linearized with describe function technique and equivalent damping coefficients are calculated. Its feasibility is examined by comparing theoretical values and experiments. Further, the proposed model is expected to be used for optimization of

designing damping characteristics of arbitrary vibration systems.

REFERENCES

1. S. Sawai, H. Okada, T. Kamo, Development of Chassis Damping Technology by Hydraulic Damper, Proceedings of 2016 JSAE annual congress(spring), No.120-14 pp19-24, 2014
2. Japan Society of Mechanical Engineer, JSME Mechanical Engineers' Handbook, Japan Society of Mechanical Engineer Vol.9 Chapter 6 p101, 2007
3. I. Kageyama, H. Yaguchi, T. Yamaguchi, Basic mechanical dynamics, Nisshin Press Chapter 8 pp113-127, 2008 (*In Japanese*)